Developing tissue specific antisense oligonucleotide-delivery to refine treatment for Duchenne muscular dystrophy

Jirka, S.

Chapter 5

Cyclic peptides to improve delivery and exon skipping of antisense oligonucleotides for Duchenne muscular dystrophy

S.M.G. Jirka[1], P.A.C. 't Hoen[1], V. Diaz Parillas[2], C. Tanganyika–de Winter[1], R.C. Verheul[2], B. Aquilera[2],

P.C. de Visser[2], A. Aartsma-Rus[1]

[1]Department of Human Genetics, Leiden University Medical Center, 2300 RC Leiden, The Netherlands

[2]BioMarin Nederland BV, 2333 CH Leiden, The Netherlands

Submitted

Abstract

Duchenne muscular dystrophy (DMD) is a severe, progressive muscle wasting disorder caused by reading frame disrupting mutations in the *DMD* gene. Exon skipping is a therapeutic approach for DMD. It employs antisense oligonucleotides (AONs) to restore the disrupted open reading frame, allowing the production of shorter, but partly functional dystrophin protein as seen in less severely affected Becker muscular dystrophy patients. To be effective, AONs need to be delivered and effectively taken up by the target cells, which can be accomplished by the conjugation of tissue homing peptides. We performed phage display screens using a cyclic peptide library combined with next generation sequencing analyses to identify candidate muscle-homing peptides. Conjugation of the lead peptide to 2′-*O*-methyl phosphorothioate AONs enabled a significant, two-fold increase in delivery and exon skipping in all analyzed skeletal and cardiac muscle of *mdx* mice and appeared well tolerated. While selected as a muscle homing peptide, uptake was increased in liver and kidney as well. The homing capacity of the peptide may have been overruled by the natural biodistribution of the AON. Nonetheless, our results suggest that the identified peptide has the potential to facilitate delivery of AONs and perhaps other compounds to skeletal and cardiac muscle.

1. Introduction

Duchenne muscular dystrophy (DMD) is a severe, progressive, X-linked muscle wasting disorder affecting 1 in 5,000 newborn boys worldwide (1,2). In general, DMD patients are diagnosed before the age of 5, become wheel-chair dependent around the age of 12, need assisted ventilation around 20 years of age and currently have a life expectancy of ~30 years in the Western world (2). DMD is caused by out of frame or nonsense mutations in the *DMD* gene that lead to truncated, non-functional dystrophin proteins. Dystrophin provides stability to the muscle fibers upon contraction (3). Lacking dystrophin, muscle fibers are easily and continuously damaged, and eventually replaced by non-functional fibrotic and adipose tissues. In contrast, Becker muscular dystrophy (BMD) is a muscle wasting disorder caused by mutations in the same gene, but here mutations maintain the open reading frame and allow production of an internally deleted, but partially functional dystrophin protein. The phenotype of patients with BMD is milder and less progressive, and patients have generally near normal life expectancies (2). Restoration of the reading frame in DMD patients would in theory allow the production of a shorter, but partly functional dystrophin protein as seen in patients with BMD (4,5). This restoration can be achieved with antisense oligonucleotides (AONs) that recognize specific exons during pre-mRNA splicing and induce skipping of target exons (6,7). The first exon skipping drug (eteplirsen) was recently approved by the FDA (http://www.fda.gov/NewsEvents/Newsroom/PressAnnouncements/ucm521263.htm).

Exon skipping AONs need to be delivered and taken up adequately by the target tissue and enter the target tissue cells to be effective. Furthermore, when taken up by endocytosis, they have to escape from the endosomes and reach the nucleus where splicing takes place. Since the human body consists of 30-40% muscle, body-wide treatment is necessary for DMD. This appeared feasible for AONs, as observed in preclinical animal studies, however in humans it remains challenging to reach a significant clinical benefit for DMD patients (6,8-12). Studies in animal models have revealed that large portions of the AON end up in liver and/or kidney, while uptake and consequently exon skipping levels in skeletal muscle and heart are low and very low, respectively when using AON doses comparable to those used in humans in clinical trials (13-15). Obviously, improved AON delivery to skeletal and cardiac muscle is anticipated to enhance therapeutic effects of AONs.

Non-muscle specific strategies for improving the delivery of AON are the use of nanoparticles, cell penetrating peptide (CPP) conjugation or co-administration of additive compounds to enhance cellular uptake (16-27). Highly cationic CPPs are, however, unsuitable for conjugation to anionic AONs such as 2′-*O*-methyl phosphorothioate AON (2OMePS) due to aggregation issues. For this AON chemistry, we therefore chose to use (non-highly cationic) tissue homing peptides, identified using phage display technology, a well-described technique to identify target specific peptides, antibodies and proteins (Smith, 1985). This approach can be cumbersome and it is well known that many false positive peptides have been identified (28). However, analyzing the outcome of phage display experiments with next generation sequencing (NGS) improves the chance of success greatly (29). NGS allows us to use just a single screening round, preventing parasitic peptide sequences to dominate the outcome and making identification of parasitic peptide sequences easier and more reliable. First encouraging results were reported using a short, linear 7-mer homing peptide selected from *in vivo* phage display biopanning experiments towards skeletal and cardiac muscle using the Ph.D.-7™ phage display library (30). This library expresses a few copies of a linear 7-mer peptide at the N-terminus of the PIII protein of the phage. In addition, a cyclic 7-mer peptide library, Ph.D.-C7C™, is available. This C7C-peptide library shares it features with the linear library but expresses peptides that are cyclized by disulfide bridges between two cysteine residues that are positioned at each end of the random 7-mer peptide. We reasoned that the conformational restriction by cyclization would lead to higher affinity binding, and thus to potentially more efficient targeting peptides.

Here, we explored the identification of muscle homing peptides with new phage display peptide library screens, *in vitro* and *in vivo*, using the Ph.D.-C7C™ peptide library combined with NGS analyses. This allowed the identification of a cyclic peptide (CyPep10) which, upon conjugation to a 2OMePS AON, resulted in a significant, two-fold increase in delivery and exon 23 skipping in all analyzed skeletal muscles and heart of the *mdx* mouse model and appeared well tolerated. Although this peptide was selected for being muscle specific, a more general increased delivery of the conjugate throughout tissues was seen. Nonetheless, results suggests that the identified peptide has the potential to facilitate targeted delivery of AONs and possible other compounds to skeletal and cardiac muscle for DMD.

2. Material and methods

Animal care

All experiments were approved by the animal experimental commission (DEC) of the LUMC and performed according to Dutch regulation for animal experimentation. Mice were housed with a 12 hour light-dark cycles in individually ventilated cages and had access to standard chow and water *ad libitum.* In all studies mice of mixed gender were used.

Cell culture

All cells were cultured in an incubator at 37ºC and 5% CO_2.

Human control myoblasts (7304-1 cells (kindly provided by dr. Vincent Mouly (31)), used for phage display biopanning) were grown in NutMix F-10 (HAM) medium supplemented with GlutaMax^{tm}-I, 20% fetal bovine serum (FBS) and 1% penicillin/streptomycin (P/S) (all from Gibco-BRL, the Netherlands) in flasks coated with purified bovine dermal collagen (collagen) for cell culture (Nutacon B.V. the Netherlands). Cells were plated on collagen coated petri-dishes and grown to 90% confluence before switching to differentiation medium (Dulbecco's medium (DMEM), without phenol red, with 2% FBS, 1% P/S, 2% GlutaMax^{tm}-I and 1% glucose (all from Gibco-BRL, the Netherlands)). Cells were allowed to differentiate for 7-14 days.

Human control myoblasts (Km155.c25 cells, kindly provided by dr. Vincent Mouly) were grown in skeletal muscle cell growth medium (Promocell, C-23160) supplemented with an extra 15% FBS and 50 µg/ml gentamicin (PAA Laboratories, USA) in uncoated flasks until 70-80% confluence was reached. Cells were plated in a six wells plate with 0.5% gelatin coated glass slides (Sigma Aldrich, the Netherlands), at a density of $1x10^5$ cells per well, 48 hours prior to differentiation. Reaching 90% confluence, medium was switched to differentiation medium (DMEM (without phenol red) with 2% FBS, 50 µg/ml gentamicin, 2% GlutaMax^{tm}-I and 1% glucose). Cells were allowed to differentiate for 3-5 days.

Immortalized human cardiomyocytes (Applied Biological Materials, Canada) were grown in Prigrow I medium supplemented with 10% FBS and 1% P/S in collagen coated flasks. Cells were plated in collagen coated glass slides in six wells plates and grown until confluence prior to experiments.

In vitro Biopanning

In vitro biopanning was performed as previously described by 't Hoen *et al* (29). Differentiated human control myoblasts cells (7304-1) were washed three times with phosphate buffered saline (PBS) and incubated with DMEM supplemented with 0.1% bovine serum albumin (BSA) for one hour at 37ºC, 5% CO_2. Cells were washed with PBS and incubated with $2x10^{11}$ phages from the Ph.D.-C7C™ Phage Display Peptide Library kit (New England Biolabs (NEB), USA) in 3 ml DMEM medium for one hour at 37ºC, while shaking at 70 rounds per minute. After incubation, the cells were gently washed six times by incubating with 5 ml of ice cold DMEM containing 0.1% BSA, for five minutes. Subsequently, the cells were incubated for 10 minutes on ice with 3 ml of 0.1M HCl (pH 2.2) to elute cell-surface bound phages, which was neutralized by addition of 0.6 ml 0.5M Tris. To recover the cell-associated phages, cells were lysed for one hour on ice in 3 ml of 30 mM Tris-HCl, 1 mM EDTA, pH 8. Phages from each fraction were titrated and amplified according to the manufacturer's instruction (NEB).

In vivo Biopanning

In total three *mdx* mice (C57Bl/10ScSn-DMD^{mdx} /J) were injected intravenously (IV) with $2x10^{11}$ phages either from the first round *in vitro* cell-surface bound phages, *in vitro* internalized phages (i.e. second selection round *in vivo*) or the naive Ph.D.-C7C™ library (i.e. first *in vivo* selection round). Phages were circulated for one hour after which mice were under anesthesia perfused with PBS. Quadriceps muscles, heart and liver were isolated from mice injected with phages from the *in vitro* selection. Gastrocnemius and quadriceps muscles, heart, liver and kidney were isolated from the mouse injected with the naive library. Tissues were homogenized in TBS buffer using a MagNalyzer according manufacturer's instruction (Roche Diagnostics, the Netherlands). Phages were titrated and amplified according to manufacturer's instruction (NEB) (from here on referred to as enriched phage library).

DNA isolation and Next Generation Sequencing

Total phage DNA was isolated from all enriched phage libraries, the naive unselected library and the naive library after a single round of bacterial amplification. From each enriched phage library, $2x10^{11}$ phage particles were added to 500 µl LB growth media in a 1.5 ml tube. The phages were precipitated with 200 µl PEG 8000/NaCl (Sigma-Aldrich, the Netherlands) for 3-4 hours at room temperature. Phages were pelleted and DNA was isolated according to the manufacturer's instruction. The final pellet (phage DNA) was dissolved in milliQ water and DNA concentration determined by Nanodrop (ThermoFisher Scientific, the Netherlands) Phage DNA was amplified by PCR using the following primers (* is a phosphorothioate bond):

Forward: AAT GAT ACG GCG ACC ACC GAG ATC TAC ACT TCC TTT AGT GGT ACC TTT CTA TTC TC*A

Reverse: CAA GCA GAA GAC GGC ATA CGA GAT CGG BARCODE TCT ATG GGA TTT TGC TAA ACA ACT TT*C

The PCR primers used to amplify the phage DNA contain a subsequence that recognized the sequence flanking the 27 nucleotides long unknown insert sequence (including the two cysteines), the adapters necessary for binding to the Illumina flow cell and a unique barcode (underlined) for every enriched phage library. The PCR protocol applied was the following: 1 ng of phage DNA was incubated with 2.625 U high fidelity Taq polymerase (Roche Diagnostics, the Netherlands), 20 pM of primers in 1 time high fidelity PCR buffer containing 15 mM $MgCl_2$, and amplified for 20 cycles, each consisting of an incubation for 30 seconds at 94°C, 30 seconds at 67°C and 30 seconds at 72°C. The PCR was stopped in exponential phase to mitigate PCR-induced sequence biases. The final PCR product was purified with the Qiaquick PCR purification kit (Qiagen, Valencia, CA, USA). Concentrations as well as the correct length of the PCR products were established with an Agilent 2100 Bioanalyzer DNA 1000 assay (Agilent Technologies, USA). All PCR products from the enriched phage libraries were combined in a single lane. Phage fractions from the naive unselected library (with and without amplification) were combined together in another lane of the Illumina flow cell. Both pools were subjected to solid phase amplification in the cluster station following manufacturer's specification (Illumina, USA). Up to 50 cycles of single end sequencing (the minimal amount required for single end sequencing in the department due to presence of unrelated samples in the other lanes) were performed using a custom sequencing primer that started exactly at the first position of the unknown insert sequence (ACA CTT CCT TTA GTG GTA CCT TTC TAT TCT CAC TC*T). Sequencing was performed with the Illumina HiSeq 2000 with a v3 flow cell and reagents (Illumina, USA).

Next generation sequencing analyses

The Illumina CASAVA 1.8.2 software was used to extract fastq files from Illumina BCL files and to split the data based on the individual sample barcodes. For further analyses, sequences were filtered out if they did not fulfill the following criteria: sequences should start with GCT TGT followed by $(NNK)_7$ and end with TGC GGT GGA GGT, with N being any nucleotide and K being G or T. Subsequently, sequences were translated to amino acid sequences with a custom perl script using conventional amino acid codon tables. When the stop codon TAG was encountered this was changed to a CAG codon according to manufacturer's instruction (NEB). An overview of the coverage is shown in supplementary table 1 and figure 1. All sequenced phage library data was normalized by a square root transformation on the number of counts in the library, a commonly applied data transformation to stabilize the variance in count data ('t Hoen et al., 2008a). Subsequently, parasitic sequences were excluded. Parasitic sequences were defined as sequences for which the frequency count in the naive amplified library minus the frequency count in the unamplified naive library was greater than two. Next, two separate analyses where performed. First, sequences with a frequency count higher than two in liver and or kidney were removed from the enriched skeletal and cardiac muscle libraries. Sequences in the skeletal and cardiac muscle libraries were, per individual enriched library, ranked by frequency count and interesting candidates divided in two groups i.e. 'skeletal muscle' and 'cardiac muscle'. Secondly, the threshold for liver and kidney was ignored and skeletal and cardiac muscle libraries ranked based on frequency count. Peptide sequences with higher frequency counts in liver and or kidney compared to skeletal or cardiac muscle were removed. Interesting candidates were selected and combined in the group 'cardiac muscle and skeletal muscle'. A final list of 25 candidate peptides was created (seven peptides for 'skeletal muscle'; seven peptides for 'cardiac muscle' and nine peptides for 'skeletal and cardiac muscle' groups). Finally, sequences with more than two positively charged amino acids (arginines or lysines) were removed from the final candidate list. Of this list, the best 12 candidate peptides were selected for further evaluation (three from 'skeletal muscle', four from 'cardiac muscle', five from 'skeletal and cardiac muscle' group)

Peptides

Fluorescently labeled cyclic and linear (Cys --> Ala substitution) peptides were obtained from Pepscan (Lelystad, the Netherlands). A FITC-label was attached to an Ahx (6-aminohexanoic acid) spacer which was added to the N-terminus of the peptide, the C-terminus was amidated and peptides were made circular by disulfide cyclization.

In vitro evaluation of FITC-labeled peptides

Positive/ negative screening. FITC-labeled peptides were dissolved in water and, if necessary, acetic acid was used to help dissolve the peptide (final acetic acid concentration in experiment <0.2% v/v.) Final peptide concentrations were determined by spectrophotometric analysis at 490 nm, pH 7.5 (~20 times diluted in 1M Tris-HCl buffer, pH 7.5)

Human control myotubes and immortalized human cardiomyocytes were washed twice with PBS and incubated with 2.25 μM of FITC-labeled peptides in serum free media for three hours at 37ºC and 5% CO_2. Cells were washed three times with PBS and fixed with cold methanol (-20ºC) for five minutes (human control myotubes) or 10 minutes (human cardiomyocytes). Subsequently the glass slides were shortly air dried, and embedded on microscope slides with Vectashield hard set containing DAPI, mounting media (Vector laboratories). After drying 30 minutes, slides were analysed with fluorescence microscopy, 20 times magnification (Leica DM5500 B) using a CCD camera (Leica DFC 360 FX).

Mechanistic uptake experiments. Human control myotubes in six-wells plate on gelatin coated cover glass slips (as previous described), were incubated for 30 minutes at 37ºC and 5% CO_2 with 7.7 μM sodium azide (NaN_3, Riedel-de Haën, Germany), 5 μg/ml chloroquine diphosphate (Sigma Aldrich, the Netherlands), 75 μg/ml fucoidan (from *focus vesiculosus*, Sigma Aldrich, the Netherlands), 2 μg/ml dextran sulfate sodium salt (Sigma Aldrich, the Netherlands), 2.5 μM chlorpromazine (Sigma Aldrich, the Netherlands), 200 μM genistein (Sigma Aldrich, the Netherlands) or were kept at 4ºC prior to the addition of 2.25 μM of FITC-labeled peptide and subsequently incubated for another three hours at 37ºC and 5% CO_2 or 4ºC in the presence of the inhibitors. Cells were washed and slides were analysed as previously described for positive/negative screening of the peptides.

AON and CyPep-AON conjugates

The 5'-carboxylate linker phosphoramidite was purchased from Link Technologies (UK). All solvents and reagents were obtained from Sigma Aldrich (the Netherlands) or Acros (Belgium) and used as received unless indicated otherwise. Cyclic peptides were synthesized by Bachem (Switzerland). Observed molecular weights were corrected for reference standard values.

AON synthesis. 2OMePS AONs modified with a 5'-carboxylate linker were prepared through standard phosphoramidite chemistry protocols, using a 2-chlorotrityl (Clt)-protected amidite for the last coupling (15eq, 20min modified coupling conditions) and final removal of the Clt group. Cleavage/ deprotection (0.1M NaOH in MeOH/H_2O 4/1 (v/v), 18h, 55^{0}C), addition of NaCl and desalting by FPLC, and subsequent lyophilization yielded the desired crude AON which was of sufficient purity to use in the next steps.

CyPep10-h45AON synthesis. The 5'-carboxylate modified h45AON (1 μmol) was added to a solution of HCTU (2.3 eq) and HOBt (2 eq) in DMSO (0.4 mL) for preactivation by shaking for three minutes at RT. CyPep10 (2 μmol and 2.3 eq DiPEA in 0.1 mL DMF) was added and the reaction mixture was shaken for one hour at RT. RP-HPLC purification was followed by salt exchange using a small excess of NaCl. Excess salt was removed by FPLC and the conjugate was evaporated to dryness three times from MilliQ, yielding CyPep10-h45AON (0.3 μmol (31%), MW (ESI) calc. 9211.9, found 9211.5).

CyPep6-23AON and CyPep10-23AON synthesis. Both conjugates were obtained through similar procedure as described for CyPep10-h45AON, in larger scale from six separate pooled syntheses: CyPep6-23AON (38 umol (37%), MW (ESI) calc. 8005.8, found 8006.5), and CyPep10-23AON (38 μmol (36%), MW (ESI) calc. 8189.1, found 8188.7)

In vitro evaluation of peptide conjugated AON

Human control myotubes (Km1555.c25, differentiated for 3-5 days) were incubated with 2 or 4 μM AON or peptide conjugated-AON (CyPep-h45AON) for 96 hours in differentiation medium without a transfection reagent. After incubation cells where washed three times with PBS and RNA was isolated by adding 500 μL TriPure (Roche diagnostics, the Netherlands) to each well to lyse the cells. This was followed by chloroform extraction in a 1/5 ratio on ice for five minutes. After centrifugation (4^{0}C, 15 minutes, 15,400 rcf) the upper aqueous phase was precipitated for 30 minutes on ice with equal volume of isopropanol. Subsequently, RNA was pelleted down by centrifugation (4°C, 15 minutes, 15,400 rcf) and the pellet washed with 70% ethanol. The final pellet (RNA) was dissolved in Milli-Q water. For complementary DNA (cDNA) synthesis, half of RNA was used in a 20 μl reaction with a specific primer reverse primer in exon 48 and transcriptor reverse transcriptase (Roche Diagnostics, the Netherlands) for 30 minutes at 55°C and five minutes at 85°C to terminate the reaction. For PCR analysis 3 μl of cDNA was incubated with 0.625 U AmpliTaq polymerase (Roche Diagnostics, the Netherlands), 10 pM of primers (reverse primer in exon 48, and a forward primer in exon 43), one time supertaq PCR buffer (Enzyme Technologies Ltd, UK) and amplified for 20 cycles each consisting of an incubation for 40 seconds at 94°C, 40 seconds at 60°C and 80 seconds at 72°C. This PCR was followed by a nested PCR in which 1.5 μl of the first PCR was incubated with 1.25 U AmpliTaq polymerase (Roche Diagnostics, the Netherlands), 20 pM of primers (reverse primer in exon 47 and a forward primer in exon 44) and one time supertaq PCR buffer (Enzyme Technologies Ltd, UK) were amplified for 32 cycles each consisting of an incubation for 40 seconds at 94°C, 40 seconds at 60°C and 60 seconds at 72°C. Exon skipping levels were semi-quantitatively determined as the percentages of the total (wild type and skipped) product with the Agilent 2100 Bioanalyzer.

In vivo evaluation of peptide conjugated AONs

hDMD mice. Four hDMD mice were injected in the gastrocnemius and triceps muscles with cardiotoxin two days prior to injection with 2.9 nmol of h45AON or CyPep10-h45AON contralateral for two consecutive days. One week after the last injection the mice were sacrificed, quadriceps (non-injected control), gastrocnemius, and triceps muscles were isolated to determine exon skip levels as described for the *in vitro* evaluation of peptide conjugated AON.

Mdx mice. Four week old (4-5 mice per group, mixed m/f) *mdx* mice (C57Bl/10ScSn-DMD^{mdx} /J) were subcutaneously (SC) injected with 50 mg/kg AON, molar equivalent of CyPep-AON, or saline four times per week for eight weeks. After the first injection, blood was collected via the tail vein to determine AON levels in plasma at 30 minutes, one hour, three hours and six hours via sparse sampling approach. One week after the last injection blood was collected via the tail vein to determine AON in plasma and assess plasma levels of markers for liver and kidney function and damage. Subsequently, mice were anesthetized, sacrificed by perfusion with PBS and gastrocnemius, quadriceps, tibialis anterior, triceps, diaphragm, heart, kidney and liver were isolated to determine exon skip, AON and dystrophin levels in tissue.

Determination of *in vivo* exon skip levels

Skeletal and cardiac muscles were homogenized in TriPure buffer (Roche Diagnostics, the Netherlands) using the MagNaLyzer and MagNaLyzer green beads (Roche Diagnostics, the Netherlands). Total RNA was isolated as described for the *in vitro* evaluation of peptide conjugated AON.

RT-PCR. cDNA was generated using 400 ng of RNA in a 20 µl reaction with random hexamer primers and transcriptor reverse transcriptase (Roche Diagnostics, the Netherlands) for 45 minutes at 42°C. For PCR analysis 1.5 µl of cDNA was incubated with 1.25 U taq polymerase (Roche Diagnostics, the Netherlands), 20 pM of primers (reverse primer in exon 24, forward primer in exon 22) and one time supertaq PCR buffer (Enzyme Technologies Ltd) and amplified for 30 cycles each consisting of an incubation for 30 seconds at 94°C, 30 seconds at 60°C and 30 seconds at 72°C. Exon skipping levels were semi-quantitatively determined as the percentages of the total (wild type and skipped) product with the Agilent 2100 Bioanalyzer.

ddPCR. cDNA was generated in 20 µl reactions, using 1,000 ng of total RNA with random hexamer primers (Roche Diagnostics, the Netherlands) and transcriptor reverse transcriptase (Roche Diagnostics, the Netherlands) according to the manufacturer's instructions. Digital droplet PCR (ddPCR) was performed in duplicate as previously described (Verheul et al., 2016) on 0.5 µl of cDNA using a Taqman assay spanning the exon 22-23 junction to detect the non-skipped fragment and an assay spanning the exon

22-24 junction to detect the skipped fragment (sequences are listed in supplementary table 2). The concentration (in copies/µl sample mix) of the skipped assay and non-skipped assay was used to calculate the percentage of exon 23 skip [copies/µl skipped/(copies/µl skipped + copies/µl non-skipped)*100].

Determination of AON levels in plasma and tissue

For measuring the concentration of (CyPep)-23AON in plasma and tissue samples a hybridization-ligation assay based on one previously published was used (Yu et al., 2002) following adaptations previously described (Jirka *et al*, 2015). Tissues were homogenized in 100 mM Tris-HCl pH 8.5, 200 mM NaCl, 0.2% SDS, 5 mM EDTA and 2 mg/mL proteinase K using MagNaLyzer green bead tubes in a MagNaLyzer (Roche Diagnostics, the Netherlands). Samples were diluted 600 and 6,000 times (muscle) or 6,000 and 60,000 (liver and kidney) in pooled control *mdx* tissue in PBS. Calibration curves of the analyzed 23AON prepared in 60 times pooled control mouse *mdx* tissue in PBS were included. All analyses were performed in duplicate. For plasma, the samples were diluted as follow: t = 30 minutes and one hour 10,000 and 100,000 times, t = three hours 1,000 and 10,000 times, t = six hours and sacrifice 100 and 1,000 times, all in pooled control plasma of *mdx* mice in PBS. Calibration curves of the analyzed 23AON prepared in 100 times pooled control plasma of *mdx* mice in PBS were included.

Determination of protein levels by western blot

Quadriceps muscle samples were homogenized in MagNaLyser green bead tubes with a MagNaLyser (Roche diagnostics, the Netherlands). Samples were homoginezed for 20 seconds at speed 7,000 (2-5 rounds) in 1 ml 125 mM Tris-HCl (pH 6.8) buffer supplemented with 20% (w/v) sodium dodecyl sulfate (SDS). Protein concentrations were determined by the bicinchoninic acid (BCA) protein assay kit (Thermo Fisher Scientific, the Netherlands) using bovine serum albumin as a standard according to manufacturer's instruction. Prior to loading, a sample volume (for muscle tissue and reference samples) representing 25 µg of total protein, was supplemented with loading buffer consisting of 125 mM Tris-HCl (pH 6.8), 20% (v/v) glycerol, 5% (v/v) β-mercaptoethanol and 0.0008% (w/v) bromophenol blue, to reach a final volume of 20 µl. Subsequently this was incubated for five minutes at 95ºC. Reference concentration samples were made by diluting total protein from wild type in *mdx* lysates of the same muscle type. Samples were loaded on Criterion XT Tris acetate (polyacrylamide) gels containing 18 slots, with a linear resolving gel gradient of 3-8% (Bio-Rad Laboratories, The Netherlands). Gels were run for one hour at 75 V (~0.07 A), followed by a two hour incubation at 150 V (~0.12 A), on ice, using XT Tricine as running buffer (Bio-Rad Laboratories B.V., the Netherlands). The gel was blotted on a nitrocellulose membrane (Bio-Rad Laboratories B.V., the Netherlands) using the ready to use Trans-Blot Turbo transfer packs

and the Trans-Blot Turbo transfer system from Bio-Rad at 2.5 A (~25 V) for 10 minutes (standard Bio-Rad protocol for high molecular weight proteins). The membrane was blocked for one hour with 5% (w/v) non-fat dried milk powder (ELK Campina Melkunie, the Netherlands) in a Tris-buffered saline buffer (TBS: 10 mM Tris-HCl (pH 8.0) and 0.15 M NaCl). Membranes were washed three times for 10 minutes with TBS-T buffer (TBS buffer with 0.005% (v/v) Tween 20) and incubated with primary antibody for dystrophin (GTX15277, 1:2000, Gene Tex, USA) and primary antibody for loading control, alpha-actinin (AB72592, 1:7500, Abcam, UK) in TBS buffer overnight at room temperature with gentle agitation. Membranes were washed three times for 15 minutes in TBS-T buffer and incubated with secondary antibody IRDye 800 CW for dystrophin (1:5000, IgG, Li-Cor, USA) and IRDye 680TL for alpha actinin (1:10000, Li-Cor, USA) in TBS buffer for one hour. Membranes were washed two times for 15 minutes in TBS-T buffer followed by a final washing step of 15 minutes in TBS buffer. Membranes were analyzed with the Odyssey system and software (Li-Cor, USA)

Safety evaluation

Blood was collected in lithium-heparin coated microvettes CB300 (Sarstedt B.V., the Netherlands). Haemoglobin (HB), urea, alkaline phosphatase (ALP), glutamate pyruvate transaminase (GPT), glutamic oxaloacetic transaminase (GOT), and creatine kinase (CK) levels were determined using Reflotron strips (Roche Diagnostics, the Netherlands) in the Reflotron Plus machine (Roche Diagnostics, the Netherlands) as previously described *(30)*.

Statistical analysis

A one-way ANOVA with a post-hoc test (Bonferroni) was used to determine significant differences in exon skipping levels, AON levels and plasma protein levels. Results were deemed significantly different when $P < 0.05$.

3. Results

Candidate peptide identification

To identify peptides that enhance the delivery of AONs to skeletal and cardiac muscle we used the Ph.D.-C7C™ phage display peptide library. A schematic outline of the screening procedure is given in figure 1. We performed a first round *in vitro* screening using human control myotubes (7304-1) in which internalized and surface bound phages were isolated and amplified. Subsequently, the naive library was also used for a first round *in vivo*, enriched internalized phage fraction and the enriched surface bound phage fraction were used for a second *in vivo* screening round in *mdx* mice, a mouse model for DMD. Gastrocnemius, quadriceps and heart were isolated for positive phage selection. Liver and kidney were isolated for negative phage selection. All enriched libraries from the biopanning selections, and the naive library with and without one round of bacterial amplification, were sequenced using a published NGS sequencing approach (29) with further adaptations and improvements to increase efficiency. First, we barcoded each of the libraries using sample specific barcodes in the reverse primer, allowing all enriched libraries to be pooled in one lane and the two naive libraries to be pooled in a second lane. Results are summarized in supplementary table 1 and supplementary figure 1.

To identify candidate peptides, the enriched phage libraries were first filtered for parasitic sequences with a propagation advantage. Sequences were considered parasitic when the frequency count in the naive amplified library minus the frequency count in the unamplified naive library was greater than two. Secondly, candidate peptides were selected based on the following criteria: A) the candidate peptide sequence has a relatively low frequency count or is absent in liver and kidney, and B) the candidate peptide sequence has either a high frequency count in skeletal muscle and low frequency count in cardiac muscle or vice versa, or C) the candidate peptide sequence has a high frequency count in both skeletal and in cardiac muscle (figure 1). Lastly, we took the charge of the peptides into account: candidate peptide sequences with more than two positively charged residues (arginines or lysines) were removed from the candidate list, because they were expected to likely form aggregates when attempting to couple them to negatively charged AONs.

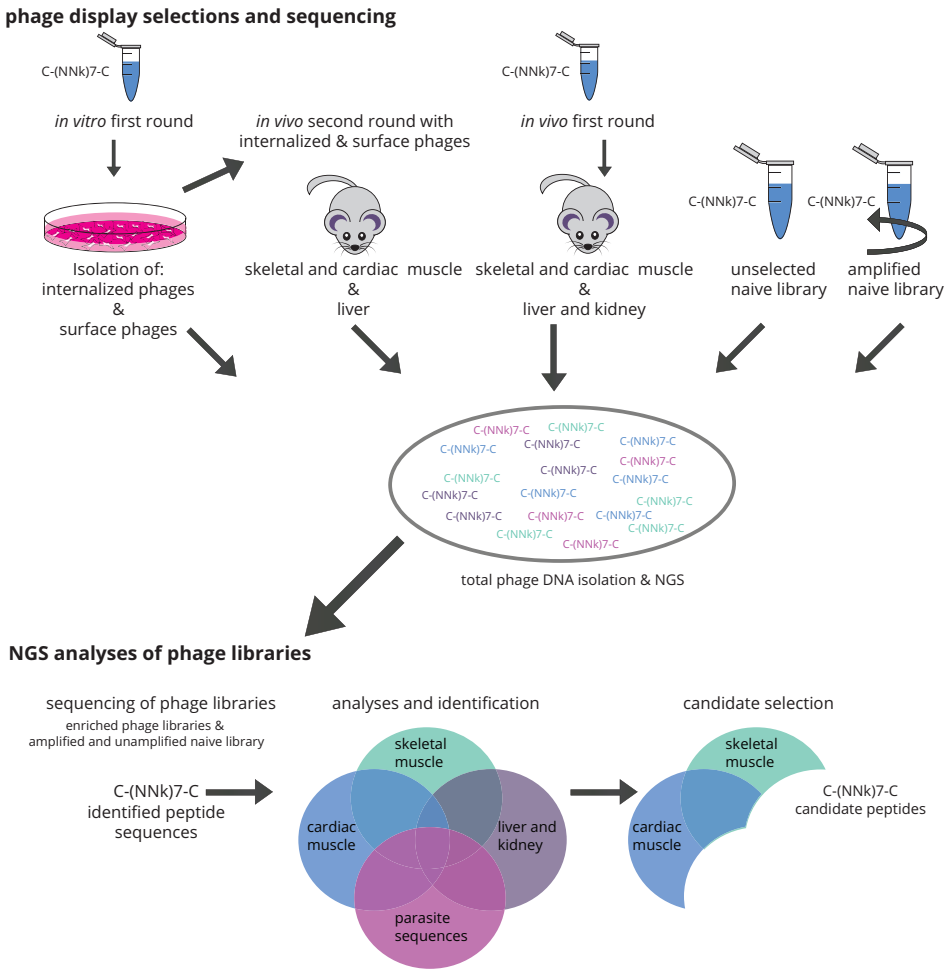

Figure1. Phage display selections and sequencing. A schematic overview of the phage display selection experiments and candidate peptide identification.

Table 1

Peptide	Sequences	Group
CyPep1	CQVRSNTTC	Muscle
CyPep2	CSLFKNFRC	Muscle/heart
CyPep3	CRADFYTTC	Heart
CyPep4	CRENTNHTC	Heart
CyPep5	CWNEDHTWC	Muscle/heart
CyPep6	CLNSLFGSC	Muscle/heart
CyPep7	CLLGHTNNC	Muscle
CyPep8	CFSHTYRVC	Muscle
CyPep9	CTYSPTEVC	Heart
CyPep10	CQLFPLFRC	Muscle/heart
CyPep11	CTLQDQATC	Heart
CyPep12	CMQHSMRVC	Muscle/heart

In vitro evaluation of the peptides

For *in vitro* evaluation of uptake by skeletal and cardiac cells, we synthesized the best 12 candidate peptides equipped with a FITC label (Table 1). Human control myotubes (km155.c25) or human cardiomyocytes cultured on cover glass slips were incubated for three hours with 2.25 µM of candidate peptides. After thorough washing, slides were fixed with methanol and embedded in mounting media containing DAPI to stain the nuclei. Most of the peptides were not taken up based on the absence of fluorescence in the cells. Cells incubated with CyPep2, CyPep8 or CyPep9 were weakly fluorescent, whereas incubation with CyPep6 (CLNSLFGSC) and CyPep10 (CQLFPLFRC) resulted in bright fluorescence throughout the cells with fluorescence also observed in the nuclei (figure 2). When we repeated the experiment using different incubation times, clear fluorescence of CyPep6 and CyPep10 could be seen in human control myotubes after one hour of incubation (figure 3a). In cardiomyocytes, higher fluorescence intensity was observed for CyPep6 compared to Cypep10 after three hours of incubation (figure 3b). Interestingly, incubation with CyPep10 resulted in detectable levels of fluorescence in human control myotubes and human cardiomyocytes cultures, already, after an incubation of 10 minutes (figure 3c), something we did not observe for CyPep6 (data not shown).

To study if the cyclisation of the peptide is crucial for the observed results, FITC-labeled linear forms of CyPep6 and 10 with Cys›Ala substitutions were synthesized. No fluorescence was observed for both peptides suggesting that not only the sequence, but also the cyclisation is responsible for the positive fluorescence observed (figure 3d).

Peptide conjugation does not impair exon skipping *in vitro* and *in vivo*

To investigate if the conjugation of these cyclic peptides to a 2OMePS AON impacts its exon skipping ability, we conjugated CyPep10 to a human AON targeting human dystrophin exon 45 (h45AON). Human control myotubes were incubated with 2 μM or 4 μM of h45AON or CyPep10-h45AON for 96 hours without a transfection reagent. Subsequently, the cells were washed, followed by RNA isolation and nested RT-PCR. Exon skipping levels were determined semi-quantitatively by lab-on-a-chip analysis. This revealed no differences in exon skipping levels (figure 4a).

Furthermore, we evaluated CyPep10-h45AON in hDMD mice, a mouse model with the human *DMD* gene integrated in the mouse genome (32). This mouse model has healthy muscle, since human dystrophin compensates for the lack of mouse dystrophin. We pretreated gastrocnemius and triceps muscles intramuscularly (IM) with cardiotoxin injections to induce muscle necrosis and enhance AON uptake (14). Two days later muscles were injected with 2.9 nmol of h45AON or a molar equivalent of CyPep10-h45AON for two consecutive days. One week after the last injection, RNA was isolated, nested RT-PCR performed and exon skipping levels were determined semi-quantitatively by lab-on-a-chip analyses. No differences in exon skipping levels were found, showing that the conjugation of a cyclic peptide to an AON also has no negative influence on its exon skipping ability *in vivo* (figure 4b).

Conjugation of CyPep10 to AONs increases uptake and exon skipping levels after systemic delivery in *mdx* mice

We evaluated CyPep6 and CyPep10 for their ability to enhance delivery and efficacy of AONs in skeletal and cardiac muscle in *mdx* mice upon systemic administration. *Mdx* mice (C57Bl/10ScSn-DMD^{mdx} /J) have a point mutation in exon 23 of the mouse *Dmd* gene, which leads to a premature stop codon, resulting in an absence of the dystrophin protein (Sicinski et al., 1989). Skipping exon 23 in the *mdx* mouse *Dmd* pre-mRNA bypasses the mutation, maintaining the reading frame and results in a shorter but (partly) functional protein. CyPep6 and CyPep10 were conjugated to a 2OMePS AON targeting the exon 23/intron 23 splice site (23AON) (33).We systemically treated four week old *mdx* mice (4-5 per group) subcutaneously (SC) for four times per week with 50 mg/kg 23AON, a molar equivalent of CyPep6-23AON or CyPep10-23AON, or saline for eight weeks. Animals were sacrificed one week after the last injection.

Evaluation of AON levels in plasma, obtained at several time-points (sparse sampling approach) after the first injection, revealed increased levels of CyPep10-23AON in plasma for the first three hours after injection but not for CyPep6-23AON (figure 5a). In tissues, a 2-fold (on average) increase of

CyPep6 and CyPep10-conjugated 23AON was observed in gastrocnemius, quadriceps, tibialis anterior and triceps muscle, and 3 and 2.8-fold increases were observed in diaphragm and heart, respectively. Unexpectedly, 2.5-fold and 3-fold increases were found in liver for CyPep6 and CyPep10 conjugated 23AON. A less prominent and non-significant 1.5 fold increase in kidney was seen for both conjugated 23AONs (figure 5b).

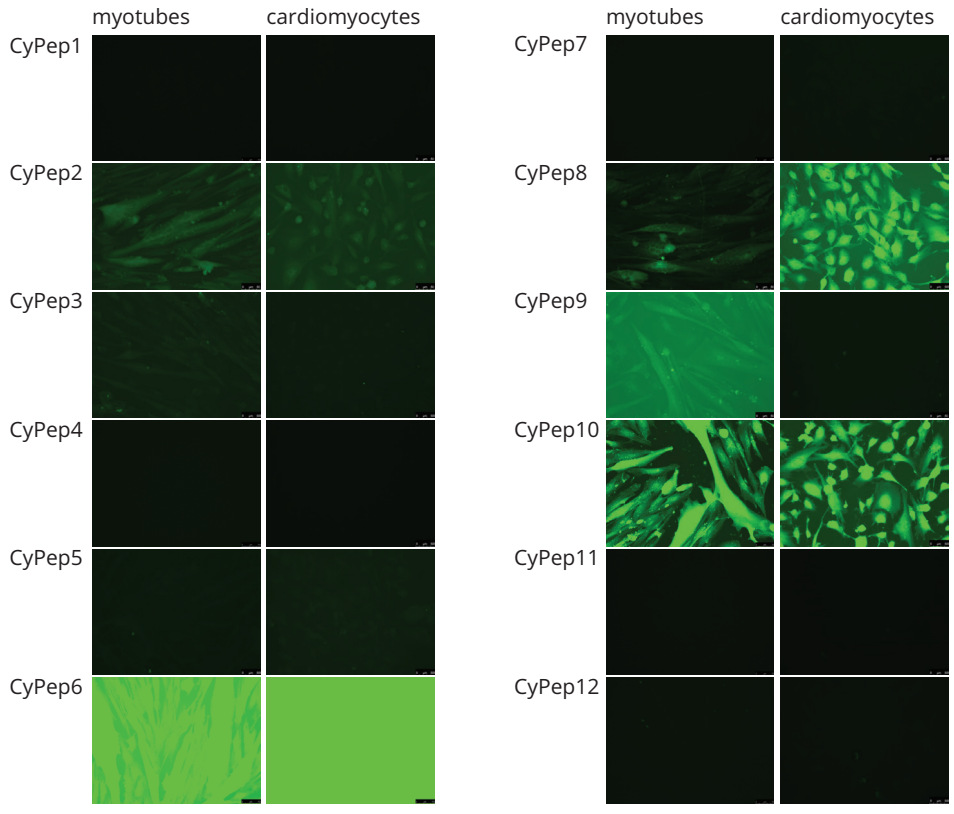

Figure 2. In vitro evaluation of fluorescently labeled cyclic-peptides. Human control myotubes and cardiomyocytes were incubated with 2.25 μM of FITC-labeled CyPeps for three hours. Slides were embedded in mounting media containing DAPI to stain nuclei. Fluorescence intensities were analyzed with fluorescence microscopy 20 times. magnification, representative pictures are shown. Bright fluorescence in the cells is seen for CyPep6 and CyPep10. CyPep2, CyPep8 and CyPep9 resulted in weak fluorescence. Scale bar = 50μm.

Exon skipping levels (single round RT-PCR) in skeletal and cardiac muscle showed a significant, 2-fold increase in exon 23 skipping for CyPep10-23AON compared to the unconjugated 23AON (figure 5c). Surprisingly,

CyPep6-23AON did not show any improvement in exon skipping levels. Dystrophin could be detected in quadriceps of all AON (conjugated and unconjugated) treated mice by western blot analysis. Upon visual inspection, a slight increase seems to be present for mice treated with CyPep10-23AON (figure 5d), but levels were too low for quantification.

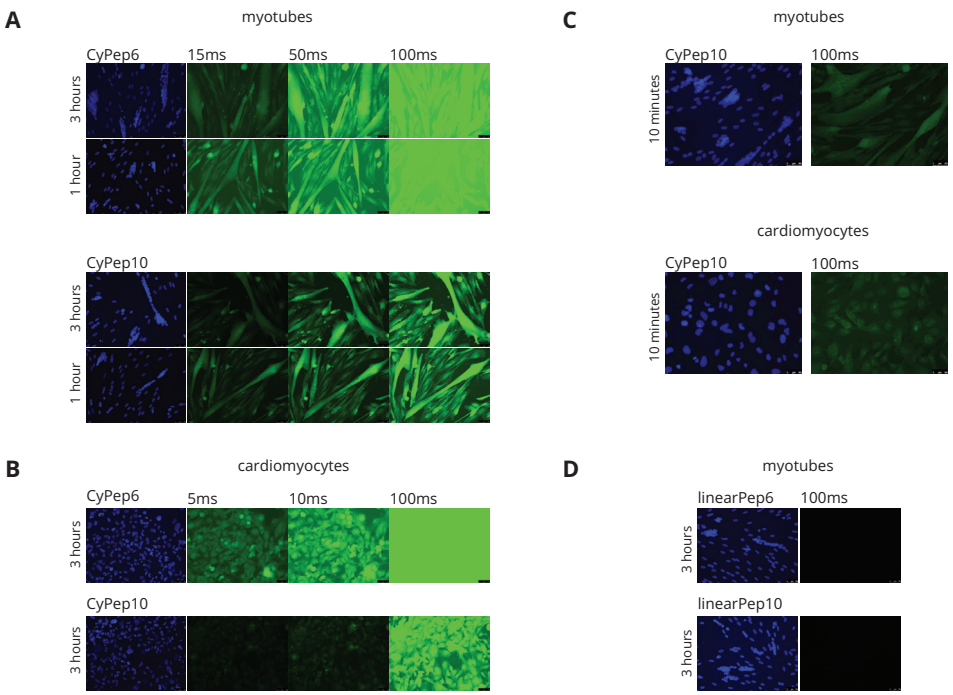

Figure 3. In vitro evaluation of CyPep6 and CyPep10. CyPep6 and CyPep10 were incubated at a dose of 2.25 µM, slides were embedded in mounting media containing DAPI and analyzed with fluorescence microscopy, 20 times magnification. a) human control myotubes incubated with CyPep6 or CyPep10 for three or one hour. b) human cardiomyocytes incubated with CyPep6 or CyPep10 for three hours. c) human control myotubes or cardiomyocytes incubated with CyPep10 for 10 minutes. d) human control myotubes incubated with linearPep6 or linearPep10 for three hours. Representative pictures are shown. First pictures (left) DAPI staining in blue, exposure time for each picture in milliseconds (ms). Scale bar = 50µm.

Results show clear fluorescence throughout the cells and in the nuclei of CyPep6 and CyPep10 at three hours and one hour of incubation for both cell lines. CyPep10 showed already positive fluorescence after 10 minutes for both cell lines. The linear forms of both peptides (with Cys -->Ala) did not show any fluorescence indicating that not only the sequence but also the cyclisation is of influence.

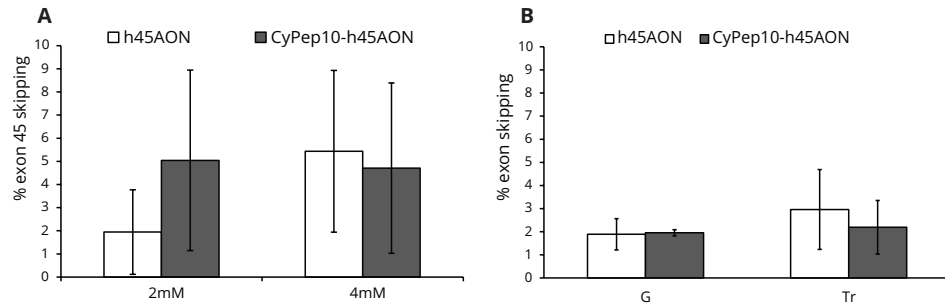

Figure 4. Evaluation of CyPep10 AON-conjugate. CyPep10 was conjugated to an AON targeting human dystrophin exon 45 (h45AON and CyPep10-h45AON) to evaluate if the conjugation of a cyclic peptide has any influence on the exon skipping functionality of the AON. a) human control myotubes incubated with 2 or 4 µM AON without any transfection reagent for 96 hours. Results show the average exon skipping levels of two independent experiments in duplo. b) IM injection in two hDMD mice (pretreated with cardiotoxin) with 2.9 nmol h45AON of molar equivalent of CyPep10-h45AON for two consecutive days. Results represent an average of two independent experiments in duplo. Results indicate that the conjugation of a cyclic peptide to a 2OMePS AON has no negative influence on the functionality of the AON. G = Gastrocnemius, Tr = Triceps. Bars represent mean ± SD.

We replicated the RT-PCR results for CyPep10-23AON for gastrocnemius, quadriceps and triceps muscles using a highly quantitative method, i.e. digital droplet PCR (ddPCR) (34). These results showed a 2.4-fold increase on average in exon 23 skipping levels for CyPep10-23AON compared to the unconjugated 23AON. This supports our findings from the RT-PCR (figure 5e).

Lastly, we evaluated blood and plasma parameters for liver and kidney damage and function to determine any possible toxicity of the conjugates used, in samples obtained just prior to sacrifice. Hemoglobin levels, urea (a marker for kidney function) and alkaline phosphatase (ALP, a marker for hepatobiliary function), showed no significant differences between groups and were within the normal range for *mdx* mice. Levels of glutamate pyruvic transaminase (GPT) and glutamic oxaloacetic pyruvate transaminase (GOT), markers for liver and muscle damage and creatine kinase (CK), marker for muscle damage, were evaluated. No significant differences were observed for GPT. GOT levels were slightly lower, but not significantly, for CyPep10-23AON. CK was significantly decreased in CyPep10-23AON treated mice compared to the 23AON, but not compared to saline treated mice due to the high variation observed in this group (supplementary figure 2).

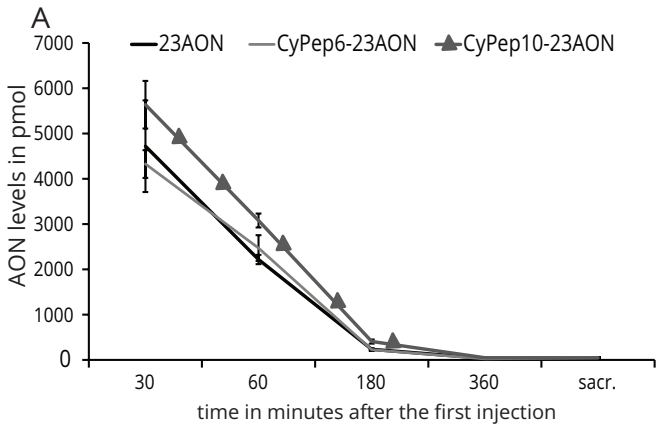

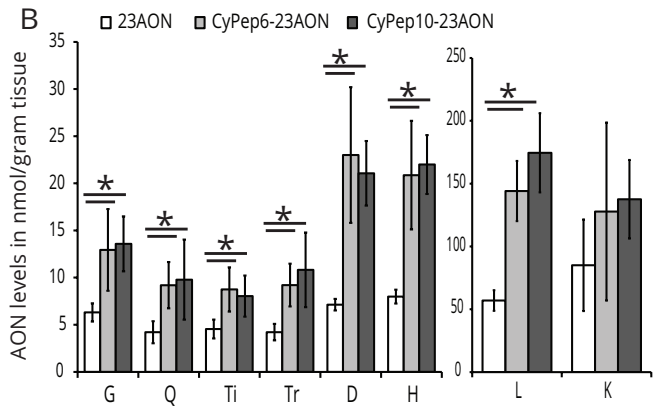

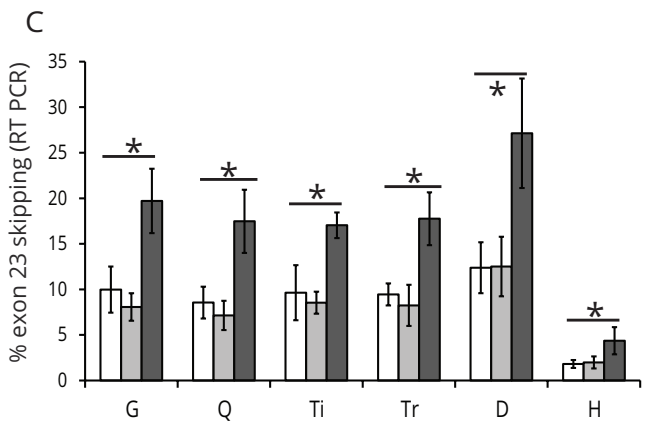

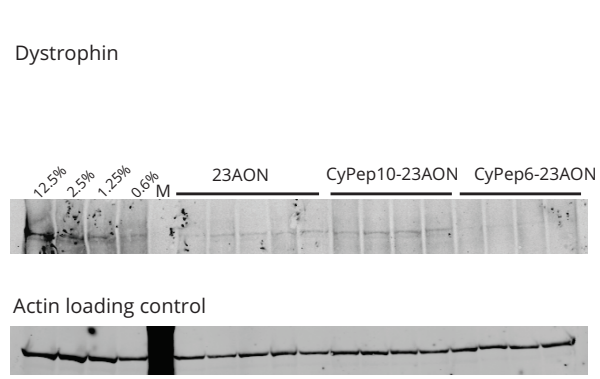

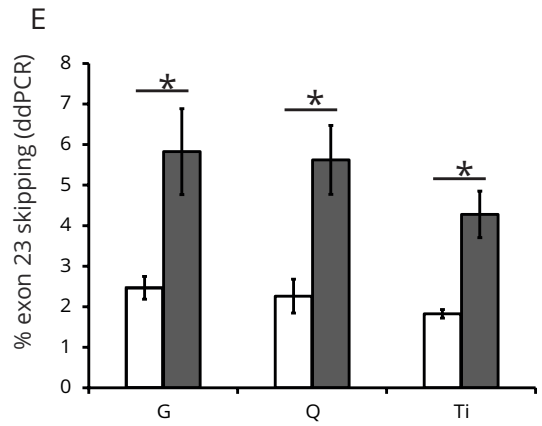

Figure 5. Systemic evaluation of CyPep6 an CyPep10 conjugated AON. Subcutaneous administration of four week old mdx mice (4-5 per group), four times per week, with 50mg/kg of 23AON, a molar equivalent of CyPep6-23AON, CyPep10-23AON or saline for eight weeks. One week after the last injection tissues were isolated. a) After the first injection blood samples were taken at several time points and at sacrifice to determine AON levels in plasma. b) A hybridization-ligation assay was used to determine AON levels in tissue. c) RNA was isolated and exon 23 skipping levels were evaluated by single RT-PCR and semi-quantitatively determined by lab-on-a-chip analysis. d) Dystrophin protein levels of quadriceps muscles were determined by western blot. e) Exon skipping levels in gastrocnemius, quadriceps and triceps muscle where quantified using ddPCR for CyPep10-23AON and 23AON treated mice. Results show an clear increase in AON levels in tissue and plasma for both peptide conjugated AON compared to the unconjugated AON. This resulted in a 2-fold increase in exon skip levels on average for CyPep10-23AON but not for CyPep6-23AON. No clear increase for dystrophin protein levels is observed. Bars represent mean ± SD. A One-way ANOVA post-hoc test (Bonferroni) used for significance (P<0.05*). G= Gastrocnemius, Q = Quadriceps, Ti = Tibialis Anterior, Tr = Triceps, D = Diaphragm, H = Heart, L = Liver, K =Kidney.

Investigation of the uptake mechanism points towards receptor mediated uptake

Encouraged by the positive results for CyPep10, we set out to study the possible uptake mechanisms for this peptide. Human control myotubes were incubated with a number of pharmacological inhibitors (Table 2) for 3.5 hours, where 2.25 µM of FITC-CyPep10 was added after 30 minutes. CyPep10 showed a clear energy dependent uptake, as no fluorescence was observed at 4ºC and reduced fluorescence was observed after pre-incubation with sodium azide. We speculate that there is no endosomal entrapment of FITC-CyPep10 based on the finding that incubation with 5 µg/ml chloroquine did not result in increased fluorescence. With fucoidan (75 µg/ml) and dextran sulfate (2 µg/ml) blocking uptake by scavenger receptors, we observed less fluorescence, suggesting that scavenger receptors are involved in the uptake of FITC-labeled CyPep10. Incubation with chlorpromazine (2.5 µM) resulted also in less fluorescence suggesting that clathrin-mediated uptake is involved. In contrast, incubation with genistein (200 µM), an inhibitor of caveolin-mediated uptake, did not shown any difference in fluorescence compared to CyPep10 alone. Combined, these results point towards an energy dependent uptake of CyPep10 via scavenger receptors accumulated in clathrin-coated pits of the muscle cell membrane (figure 6).

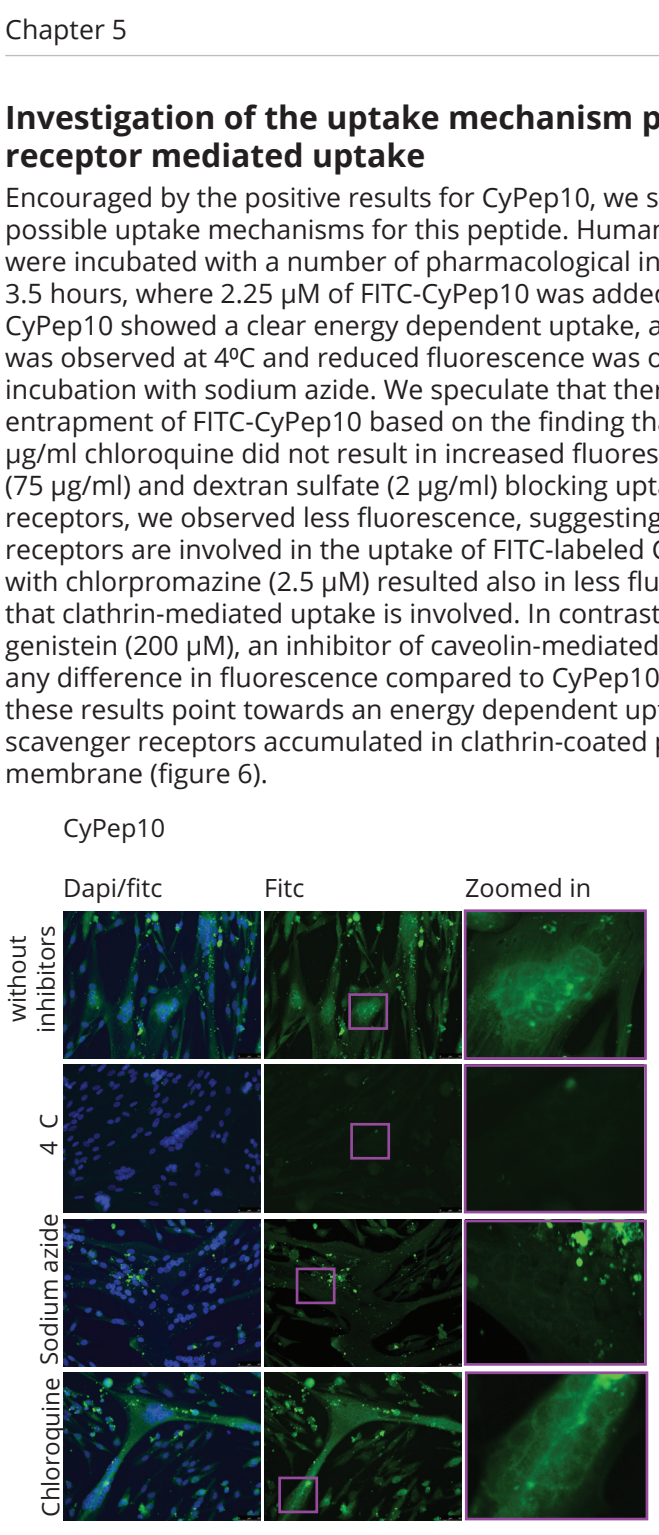

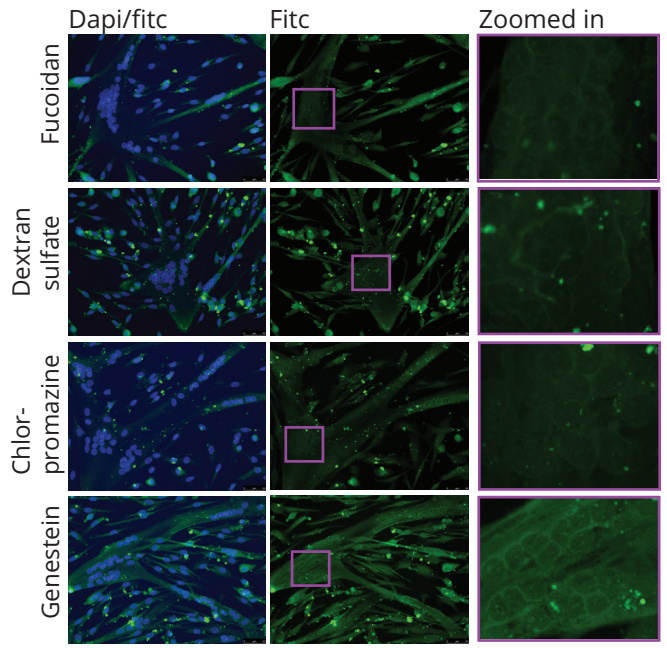

Figure 6. Uptake mechanism of CyPep10. Human control myotubes were incubated with pharmacological inhibitors for 30 minutes prior to a three hour incubation with CyPep10 in the presence of the inhibitors. Results were analyzed with fluorescence microscopy. Representative pictures are shown scale bar = 50 µm.

4. Discussion

Exon skipping is a therapeutic approach for DMD. Improved delivery of AON to the target tissue is anticipated to increase the therapeutic effect. Achieving this in a safe and effective way is challenging, although some progress has been made using PCM polymers, or ZM2 or polymeric nanoparticles (22,23,35). Most progress to increase the delivery and efficacy has been achieved by the conjugation of arginine rich cell penetrating peptides to non-anionic AONs such as peptide nucleic acid (PNA) and phosphorodiamidate morpholino oligomer (PMO). It was found that some of these highly cationic peptides were poorly tolerated in higher animals due to kidney toxicity (25). A different approach is the use of tissue homing peptides, which are not necessarily highly cationic. In 1999, Samoylova *et al.,* described a phage, expressing the 7-mer peptide ASSLNIA, which showed increased fluorescence in murine tissues compared to control phages upon histochemical analyses. Unfortunately, the peptide alone was unable to increase delivery or exon skipping levels in *mdx* mice when conjugated to a PMO (36,37). More recently, Gao *et al.,* reported the M12

peptide RRQPPRSISSHP (38), which, upon conjugation to a PMO, resulted in improved but variable exon skipping levels in *mdx* mice in skeletal muscle but not heart. Previously we described the 7-mer P4 peptide LGAQSNF identified through phage display studies, which, upon conjugation to a 2OMePS AON, resulted in significantly increased exon skipping levels in diaphragm and cardiac muscle tissue of *mdx* mice (30). Taken together, tissue homing peptide conjugation to AONs appears to be a promising strategy.

We believe the approach we have used here (figure 1) facilitates the identification of effective muscle homing peptides from phage display studies further for several reasons. First, as already outlined by other studies (29,39-41), the use of NGS enables to study large numbers of sequences. By sequencing the naive library before and after one round of bacterial amplification one can identify library specific peptide sequences that are overrepresented or have an amplification bias, the so called parasite sequences (29,41). With our approach we assessed that a little over 1.9 million unique sequences in the naive amplified library are potentially parasitic sequences (around 21% of the total library). In the enriched libraries, ~11% of the unique sequences were represented by these parasitic sequences. However, even with NGS, only a fraction of possible sequences in the enriched libraries are sequenced (for comparison, the naive library contains $1.28x10^9$ unique sequences whereas we sequenced approximately $1\text{-}2.5x10^6$ sequences of the enriched libraries). Nevertheless, these millions of sequences are a vast improvement over the ~50-100 phage clones generally sequenced with Sanger sequencing (30). Furthermore, many sequences in the enriched library will be present only once or twice with the more abundant sequences primarily being of interest. As such, NGS sequencing will generally provide sufficient depth to identify interesting candidates. Additionally, the databases Pepbank (42) and Sarotup (28) can be used to filter known parasitic sequences or target-unrelated sequences, but are mainly applicable to linear peptides and do not provide sufficient information about cyclic peptides. Secondly, combining a first round *in vitro* screening with a second selection round *in vivo* screening we aimed to increase the potential binding of peptides towards muscle, since peptides with no affinity towards muscle would be deselected in the first round. By isolating phages from liver and kidney we were able to filter peptides which predominately were taken up by these tissues (e.g. target-unrelated sequences).

The 12 selected candidate peptides contained a group of seven that were identified in either skeletal or cardiac muscle (data not shown) and a group of five that were identified in both skeletal and cardiac muscle. *In vitro* evaluation of these candidates in human myotubes and cardiomyocyte cultures left us with two peptides for further study: CyPep6 and CyPep10, both identified in skeletal and cardiac muscle. Interestingly, of the peptides

selected based on presence in skeletal muscle or cardiac muscle, only three out of seven showed some degree of fluorescence. While in the group selected based on presence in skeletal and cardiac muscles, two out of three showed bright fluorescence and one showed some fluorescence. This suggests that for future studies it may be more efficient to focus only on peptides enriched in both skeletal and cardiac muscle tissue.

Systemic administration of CyPep6 and CyPep10-conjugated 23AON in *mdx* mice revealed a 2-fold increase of AON levels in skeletal muscle and around three-fold increase in diaphragm muscle and heart for both peptide conjugates over the unconjugated 23AON. This resulted in a significant 2-fold increase in exon skipping in all tissues analyzed for CyPep10-23AON, but surprisingly not for CyPep6-23AON (figure 5). A potential explanation for the discrepancy between CyPep6-23AON tissue levels and activity may lie in the fact that the peptides were isolated from muscle and heart tissue homogenates, and not selected for their capacity to actually enter the tissue or tissue cells. It is therefore possible that CyPep6-23AON conjugate is trapped somewhere in the endothelium or interstitium. Judged on the fluorescence observed *in vitro*, CyPep6 outperformed CyPep10 for both cell lines at time points one and three hours, except for the 10 minute incubation time point (figure 3). CyPep6 appears to be taken up by cells efficiently however not as fast as CyPep10. This could indicate that different mechanistic uptake pathways are involved and that fast uptake *in vitro* might lead to a better outcome *in vivo*. If CyPep6 alone does enter tissue and tissue cells, conjugation to the larger AON may have negatively affected the tissue- or cellular uptake *in vivo*. The fact that CyPep10-23AON did show increased exon skip levels suggests that this peptide conjugate is taken up by the target cells efficiently. Unfortunately, dystrophin levels were very low and could not be accurately quantified. It is known that dystrophin levels accumulate for 12-24 weeks after treatment initiation (43), so the time of sacrifice (deemed optimal for analysis of AON and exon skipping levels) is probably not optimal for assessing dystrophin levels.

Compared to unconjugated AON, we observed for CyPep10-23AON similar uptake in kidney, but a 2.5-fold increase in AON levels in liver. No clear indication is found in our NGS data that could explain the increased uptake in liver. CyPep10 showed a 4-fold increase in frequency count in the second round *in vivo* in quadriceps and heart compared to the first round *in vitro* (internalized phage fraction). Frequency counts in liver were 2.5 times lower in the second selection round *in vivo* compared to quadriceps and heart. After the first selection round *in vivo*, the counts in liver were 6.5 times lower compared to heart and 1.5 times lower compared to kidney. Thus the kidney and liver levels of CyPep10-AON conjugate may seem surprising given that the peptide was selected based on low uptake in these organs. However, one should not forget that the identified peptide was conjugated, in multiple copies, to a phage, while now it is singly conjugated to a 2OMePS

AON, which is by itself taken up efficiently by liver and kidney. It is not unlikely that this is further facilitated by peptide conjugation and/or that increased levels are due to the increased plasma half-life.

We finally investigated the mechanism by which FITC-labelled CyPep10 is taken up. Results clearly show that uptake of CyPep10 by muscle cells is energy dependent, because incubation at 4ºC or with an ATP inhibitor almost completely prevented uptake. The involvement of scavenger receptors accumulated in clathrin-coated pits is also implied, since uptake was inhibited by inhibitors of scavenger receptors and clathrin-mediated uptake. Clathrin-mediated uptake is one of the main and best studied uptake pathways (44). It requires strong receptor/-ligand binding and clustering in clathrin-coated pits in an energy dependent way. The clathrin-coated pits invaginate and pinch off from the membrane into clathrin-coated vesicles, which later on form early and late endosomes. Subsequently, ligand and receptors are sorted and transported to their appropriated cellular destination such as, Golgi Apparatus, liposomes, nucleus or back to the cell membrane. Endosomes appear to play a role after the peptide enters the cell in clathrin–coated vesicles. This is supported by the fact that pre-incubation with chloroquine, an inhibitor of endosomal entrapment, did not result in a clear increase in fluorescence.

In conclusion, we have identified CyPep10 from phage display studies, as a potential candidate for AON delivery. Although this peptide was selected as muscle specific, upon conjugation to the AON, the conjugate showed general improved tissue levels in a mouse model for DMD. Extended studies will be needed to assess if long term treatment leads to beneficial effects on muscle quality and function.

Acknowledgements

We hereby thank de following people for their technical or intellectual input: M. van Putten, J.W. Boertje- van der Meulen, M. Hulsker, L. van Vliet, M. Overzier, A. Harder (student) employed by the LUMC, Leiden the Netherlands. D. Muilwijk, K.H. Pang, R. Vermue, N.A. Datson and J.C.T. van Deutekom employed by BioMarin Nederland BV, Leiden the Netherlands.

Studies were financed by the Dutch Ministry of Economic Affairs to PH (IOP-Genmics grant IGE7001) and a grant from the Prinses Beatrix Spierfonds to AAR (W-OR13-06).

Author disclosure statement

AAR is co-inventor of patents of the LUMC on exon skipping, licensed by LUMC to Prosensa Therapeutics, and being entitled to a share or royalties. SJ, AAR, PH, BA and PCdV are co-inventors on a patent that include the peptides reported in this work. AAR also declares being an ad hoc consultant for Global Guidepoint, GLC consulting, Deerfield Institute, Bioclinica, Grunenthal, Summit PLC, PTC Therapeutics and BioMarin and being a member of the scientific advisory board of ProQR and Philae Pharmaceuticals. Remuneration for these activities go to LUMC. PCdV, RCV BA and VDP are employees of BioMarin Nederland BV.

References

1. Moat, S.J., Bradley, D.M., Salmon, R., Clarke, A. and Hartley, L. (2013) Newborn bloodspot screening for Duchenne muscular dystrophy: 21 years experience in Wales (UK). *Eur.J.Hum.Genet.*

2. Emery, A.E. (2002) The muscular dystrophies. *Lancet*, **359**, 687-695.

3. Blake, D.J., Weir, A., Newey, S.E. and Davies, K.E. (2002) Function and genetics of dystrophin and dystrophin-related proteins in muscle. *Physiol Rev.*, **82**, 291-329.

4. Monaco, A.P., Bertelson, C.J., Liechti-Gallati, S., Moser, H. and Kunkel, L.M. (1988) An explanation for the phenotypic differences between patients bearing partial deletions of the DMD locus. *Genomics*, **2**, 90-95.

5. Muntoni, F., Torelli, S. and Ferlini, A. (2003) Dystrophin and mutations: one gene, several proteins, multiple phenotypes. *The Lancet. Neurology*, **2**, 731-740.

6. Aartsma-Rus, A., Janson, A.A., Kaman, W.E., Bremmer-Bout, M., den Dunnen, J.T., Baas, F., van Ommen, G.J. and van Deutekom, J.C. (2003) Therapeutic antisense-induced exon skipping in cultured muscle cells from six different DMD patients. *Hum.Mol.Genet.*, **12**, 907-914.

7. Aartsma-Rus, A. (2010) Antisense-mediated modulation of splicing: therapeutic implications for Duchenne muscular dystrophy. *RNA.Biol.*, **7**, 453-461.

8. Aartsma-Rus, A. (2014) Dystrophin analysis in clinical trials. *JND*, **1**, 41-53.

9. Flanigan, K.M., Voit, T., Rosales, X.Q., Servais, L., Kraus, J.E., Wardell, C., Morgan, A., Dorricott, S., Nakielny, J., Quarcoo, N. *et al.* (2014) Pharmacokinetics and safety of single doses of drisapersen in non-ambulant subjects with Duchenne muscular dystrophy: results of a double-blind randomized clinical trial. *Neuromuscul.Disord.*, **24**, 16-24.

10. Voit, T., Topaloglu, H., Straub, V., Muntoni, F., Deconinck, N., Campion, G., de Kimpe, S.J., Eagle, M., Guglieri, M., Hood, S. *et al.* (2014) Safety and efficacy of drisapersen for the treatment of Duchenne muscular dystrophy (DEMAND II): an exploratory, randomised, placebo-controlled phase 2 study. *Lancet Neurol.*, **13**, 987-996.

11. Mendell, J.R., Rodino-Klapac, L.R., Sahenk, Z., Roush, K., Bird, L., Lowes, L.P., Alfano, L., Gomez, A.M., Lewis, S., Kota, J. *et al.* (2013) Eteplirsen for the treatment of Duchenne muscular dystrophy. *Ann. Neurol.*, **74**, 637-647.

12. Fall, A.M., Johnsen, R., Honeyman, K., Iversen, P., Fletcher, S. and Wilton, S.D. (2006) Induction of revertant fibres in the mdx mouse using antisense oligonucleotides. *Genetic vaccines and therapy*, **4**, 3.

13. Heemskerk, H.A., de Winter, C.L., de Kimpe, S.J., van Kuik-Romeijn, P., Heuvelmans, N., Platenburg, G.J., van Ommen, G.J., van Deutekom, J.C. and Aartsma-Rus, A. (2009) In vivo comparison of 2'-O-methyl phosphorothioate and morpholino antisense oligonucleotides for Duchenne muscular dystrophy exon skipping. *J.Gene Med.*, **11**, 257-266.

14. Heemskerk, H., de Winter, C., van Kuik, P., Heuvelmans, N., Sabatelli, P., Rimessi, P., Braghetta, P., van Ommen, G.J., de, K.S., Ferlini, A. *et al.* (2010) Preclinical PK and PD studies on 2'-O-methyl-phosphorothioate RNA antisense oligonucleotides in the mdx mouse model. *Mol.Ther.*, **18**, 1210-1217.

15. Wu, B., Xiao, B., Cloer, C., Shaban, M., Sali, A., Lu, P., Li, J., Nagaraju, K., Xiao, X. and Lu, Q.L. (2011) One-year treatment of morpholino antisense oligomer improves skeletal and cardiac muscle functions in dystrophic mdx mice. *Mol.Ther.*, **19**, 576-583.

16. Hu, Y., Wu, B., Zillmer, A., Lu, P., Benrashid, E., Wang, M., Doran, T., Shaban, M., Wu, X. and Lu, Q.L. (2010) Guanine analogues enhance antisense oligonucleotide-induced exon skipping in dystrophin gene in vitro and in vivo. *Mol.Ther.*, **18**, 812-818.

17. Verhaart, I.E. and Aartsma-Rus, A. (2012) The effect of 6-thioguanine on alternative splicing and antisense-mediated exon skipping treatment for duchenne muscular dystrophy. *PLoS.Curr.*, **4**.

18. Kendall, G.C., Mokhonova, E.I., Moran, M., Sejbuk, N.E., Wang, D.W., Silva, O., Wang, R.T., Martinez, L., Lu, Q.L., Damoiseaux, R. *et al.* (2012) Dantrolene enhances antisense-mediated exon skipping in human and mouse models of Duchenne muscular dystrophy. *Sci.Transl.Med.*, **4**, 164ra160.

19. Rimessi, P., Sabatelli, P., Fabris, M., Braghetta, P., Bassi, E., Spitali, P., Vattemi, G., Tomelleri, G., Mari, L., Perrone, D. *et al.* (2009) Cationic PMMA nanoparticles bind and deliver antisense oligoribonucleotides allowing restoration of dystrophin expression in the mdx mouse. *Mol. Ther.*, **17**, 820-827.

20. Mumcuoglu, D., Sardan, M., Tekinay, T., Guler, M.O. and Tekinay, A.B. (2015) Oligonucleotide delivery with cell surface binding and cell

penetrating Peptide amphiphile nanospheres. *Mol.Pharm.*, **12**, 1584-1591.

21. Ferlini, A., Sabatelli, P., Fabris, M., Bassi, E., Falzarano, S., Vattemi, G., Perrone, D., Gualandi, F., Maraldi, N.M., Merlini, L. *et al.* (2010) Dystrophin restoration in skeletal, heart and skin arrector pili smooth muscle of mdx mice by ZM2 NP-AON complexes. *Gene Ther.*, **17**, 432-438.

22. Bassi, E., Falzarano, S., Fabris, M., Gualandi, F., Merlini, L., Vattemi, G., Perrone, D., Marchesi, E., Sabatelli, P., Sparnacci, K. *et al.* (2012) Persistent dystrophin protein restoration 90 days after a course of intraperitoneally administered naked 2'OMePS AON and ZM2 NP-AON complexes in mdx mice. *J.Biomed.Biotechnol.*, **2012**, 897076.

23. Wang, M., Wu, B., Lu, P., Cloer, C., Tucker, J.D. and Lu, Q. (2013) Polyethylenimine-modified pluronics (PCMs) improve morpholino oligomer delivery in cell culture and dystrophic mdx mice. *Mol.Ther.*, **21**, 210-216.

24. Lehto, T., Castillo, A.A., Gauck, S., Gait, M.J., Coursindel, T., Wood, M.J., Lebleu, B. and Boisguerin, P. (2013) Cellular trafficking determines the exon skipping activity of Pip6a-PMO in mdx skeletal and cardiac muscle cells. *Nucleic Acids Res.*

25. Moulton, H.M. and Moulton, J.D. (2010) Morpholinos and their peptide conjugates: therapeutic promise and challenge for Duchenne muscular dystrophy. *Biochim.Biophys.Acta*, **1798**, 2296-2303.

26. Yin, H., Saleh, A.F., Betts, C., Camelliti, P., Seow, Y., Ashraf, S., Arzumanov, A., Hammond, S., Merritt, T., Gait, M.J. *et al.* (2011) Pip5 transduction peptides direct high efficiency oligonucleotide-mediated dystrophin exon skipping in heart and phenotypic correction in mdx mice. *Mol.Ther.*, **19**, 1295-1303.

27. Betts, C.A., Saleh, A.F., Carr, C.A., Hammond, S.M., Coenen-Stass, A.M., Godfrey, C., McClorey, G., Varela, M.A., Roberts, T.C., Clarke, K. *et al.* (2015) Prevention of exercised induced cardiomyopathy following Pip-PMO treatment in dystrophic mdx mice. *Sci.Rep.*, **5**, 8986.

28. Huang, J., Ru, B., Li, S., Lin, H. and Guo, F.B. (2010) SAROTUP: scanner and reporter of target-unrelated peptides. *J.Biomed.Biotechnol.*, **2010**, 101932.

29. 't Hoen, P.A., Jirka, S.M., Ten Broeke, B.R., Schultes, E.A., Aguilera, B., Pang, K.H., Heemskerk, H., Aartsma-Rus, A., van Ommen, G.J. and den Dunnen, J.T. (2012) Phage display screening without repetitious

selection rounds. *Anal.Biochem.*, **421**, 622-631.

30. Jirka, S.M., Heemskerk, H., Tanganyika-de Winter, C.L., Muilwijk, D., Pang, K.H., de Visser, P.C., Janson, A., Karnaoukh, T.G., Vermue, R., 't Hoen, P.A. *et al.* (2013) Peptide Conjugation of 2'-O-methyl Phosphorothioate Antisense Oligonucleotides Enhances Cardiac Uptake and Exon Skipping in mdx Mice. *Nucleic Acid Ther.*

31. Zhu, C.H., Mouly, V., Cooper, R.N., Mamchaoui, K., Bigot, A., Shay, J.W., Di Santo, J.P., Butler-Browne, G.S. and Wright, W.E. (2007) Cellular senescence in human myoblasts is overcome by human telomerase reverse transcriptase and cyclin-dependent kinase 4: consequences in aging muscle and therapeutic strategies for muscular dystrophies. *Aging Cell*, **6**, 515-523.

32. 't Hoen, P.A., de Meijer, E.J., Boer, J.M., Vossen, R.H., Turk, R., Maatman, R.G., Davies, K.E., van Ommen, G.J., van Deutekom, J.C. and den Dunnen, J.T. (2008) Generation and characterization of transgenic mice with the full-length human DMD gene. *J.Biol.Chem.*, **283**, 5899-5907.

33. Mann, C.J., Honeyman, K., McClorey, G., Fletcher, S. and Wilton, S.D. (2002) Improved antisense oligonucleotide induced exon skipping in the mdx mouse model of muscular dystrophy. *J.Gene Med.*, **4**, 644-654.

34. Verheul, R.C., van Deutekom, J.C. and Datson, N.A. (2016) Digital Droplet PCR for the Absolute Quantification of Exon Skipping Induced by Antisense Oligonucleotides in (Pre-)Clinical Development for Duchenne Muscular Dystrophy. *PloS one*, **11**, e0162467.

35. Falzarano, M.S., Bassi, E., Passarelli, C., Braghetta, P. and Ferlini, A. (2014) Biodistribution studies of polymeric nanoparticles for drug delivery in mice. *Hum.Gene Ther.*, **25**, 927-928.

36. Samoylova, T.I. and Smith, B.F. (1999) Elucidation of muscle-binding peptides by phage display screening. *Muscle Nerve*, **22**, 460-466.

37. Yin, H., Moulton, H.M., Betts, C., Seow, Y., Boutilier, J., Iverson, P.L. and Wood, M.J. (2009) A fusion peptide directs enhanced systemic dystrophin exon skipping and functional restoration in dystrophin-deficient mdx mice. *Hum.Mol.Genet.*, **18**, 4405-4414.

38. Gao, X., Zhao, J., Han, G., Zhang, Y., Dong, X., Cao, L., Wang, Q., Moulton, H.M. and Yin, H. (2014) Effective dystrophin restoration by a novel muscle-homing peptide-morpholino conjugate in dystrophin-deficient mdx mice. *Mol.Ther.*, **22**, 1333-1341.

39. Dias-Neto, E., Nunes, D.N., Giordano, R.J., Sun, J., Botz, G.H., Yang, K., Setubal, J.C., Pasqualini, R. and Arap, W. (2009) Next-generation phage display: integrating and comparing available molecular tools to enable cost-effective high-throughput analysis. *PLoS.One.*, **4**, e8338.

40. McLaughlin, M.E. and Sidhu, S.S. (2013) Engineering and analysis of peptide-recognition domain specificities by phage display and deep sequencing. *Methods Enzymol.*, **523**, 327-349.

41. Matochko, W.L., Cory, L.S., Tang, S.K. and Derda, R. (2014) Prospective identification of parasitic sequences in phage display screens. *Nucleic Acids Res.*, **42**, 1784-1798.

42. Shtatland, T., Guettler, D., Kossodo, M., Pivovarov, M. and Weissleder, R. (2007) PepBank--a database of peptides based on sequence text mining and public peptide data sources. *BMC.Bioinformatics.*, **8**, 280.

43. Verhaart, I.E., Dool, v.V.-v.d., Sipkens, J.A., de Kimpe, S.J., Kolfschoten, I.G., van Deutekom, J.C., Liefaard, L., Ridings, J.E., Hood, S.R. and Aartsma-Rus, A. (2014) The Dynamics of Compound, Transcript, and Protein Effects After Treatment With 2OMePS Antisense Oligonucleotides in mdx Mice. *Mol.Ther.Nucleic Acids*, **3**, e148.

44. McMahon, H.T. and Boucrot, E. (2011) Molecular mechanism and physiological functions of clathrin-mediated endocytosis. *Nat.Rev.Mol. Cell Biol.*, **12**, 517-533.